Received: 24 December 2020 | Revised: 13 February 2021 | Accepted: 23 February 2021

DOI: 10.1002/aoc.6225

FULL PAPER

Applied Organometallic Chemistry WILEY

New advances in catalytic performance of erbium-folic acid-coated $CoFe_2O_4$ complexes for green one-pot three-component synthesis of pyrano[2,3-*d*]pyrimidinone and dihydropyrano[3,2-*c*]chromenes compounds in water

Serve Sorkhabi | **Roya Mozafari** | **Mohammad Ghadermazi**

Department of Chemistry, Faculty of Science, University of Kurdistan, Sanandaj, Iran

Correspondence
Mohammad Ghadermazi, Department of Chemistry, Faculty of Science, University of Kurdistan, Sanandaj, Iran.
Email: mghadermazi@uok.ac.ir

Funding information
University of Kurdistan

In the current research, much attention is paid to heterogenized nanostructure. Herein, we report the green synthesis magnetic nanoparticles (MNPs) of cobalt ferrite by the immobilization of erbium (Er) coated with folic acid (FA) which show effective catalytic properties and recyclability. Full characterizations with field emission scanning electron microscopy (FE-SEM), transmission electron microscopy (TEM), energy-dispersive X-ray spectroscopy (EDX), X-ray atomic mapping, thermal gravimetric analysis (TGA), X-ray diffraction (XRD), vibrating sample magnetometer (VSM), **i**nductively coupled plasma-optical emission spectrometry (ICP-OES), and Fourier-transform infrared (FT-IR) spectroscopy techniques were undertaken to uncover structural properties of the prepared magnetic catalyst. The obtained nanohybrid complexes as efficient, recyclable, and green heterogeneous systems pave the way for producing pyrano[2,3-*d*]pyrimidinone and dihydropyrano[3,2-*c*]chromenes derivatives by the one-pot three-component condensation reaction of various aldehydes, malononitrile, and hydroxycoumarin or barbituric acid in green condition. This easily prepared organometalic catalyst presents many superiorities such as operational simplicity, high yield, short reaction time, utilization of commercially available or easily accessible starting materials, eco-friendly properties, and excellent purity. Most importantly, erbium-FA-coated $CoFe_2O_4$ can be easily separated and recycled from the reaction system using an external magnetic field. The magnetically recoverable biocatalyst can be recycled and reused six times while maintaining high activities. The activity of the magnetic catalyst can be maintained at more than 80% of that of the previous cycle. This research solves the recovery problem encountered in industrial applications of biocatalysts and presents a clean and green method for preparing pyrimidinones and chromenes.

KEYWORDS
chromenes, eco-friendly chemistry, folic acid, magnetic nanocatalyst, pyrimidinone

1 | INTRODUCTION

Today, the efficient synthesis of chemicals can be characterized, not only by main factors as overall yield and selectivity but also by its time, human resources, using natural compounds, and the amount of required energy and imposed hazards and also toxicity of the relevant compounds and systems.[1] Multicomponent reactions (MCRs) have been presented as a powerful and affective way in new chemistry due to fast and easy availability of substrates without separation of any intermediate.[2–7] Moreover, by using multiple transformations, the approach of MCRs is extremely congruous with the goals of "green chemistry."[8,9]

Also, using MCRs in an aqueous condition is an active scope of investigation for modern combinatorial chemists and medicinal combinatorial chemists due to the simple design of reaction, lower cost, powerful bond forming, efficiency, being devoid of any carcinogenic effects, atom economy, diversity-oriented synthesis (DOS), reduced environmental challenges, and the simplicity to synthesis target materials by the use of several proper elements that are valuable to the environment and to the industry.[10,11]

Pyran rings are normal structural subunits which exist in several natural compounds, such as alkaloids, carbohydrates, iridoids, pheromones, and polyether antibiotics.[12,13] Recently, these organic structures have attracted remarkable interest because of their numerous biological functions. Owing to bio-isosteric parameters, aromatic six-membered *N*-heterocyclic structures are of much significance in the pharmaceutical points of view both practically and theoretically. For example, pyrimidine rings as a basic part of RNA and DNA have a considerable role in various biological functions.[14–16] Hence, the chemotherapeutic influence of annulated pyrano[2,3-*d*]pyrimidines is due to their potency to inhibit enzyme activity toward DNA preparation, including thymidylate synthetase (TSase), dihydrofolate reductase (DHFR), reverse transcriptase (RTase), and thymidine phosphorylase (TPase).[17] When pyrano [2,3-*d*]pyrimidine derivatives are annulated into a target location, the outcome compound increases pharmaceutical ability, such as antileishmanial activity,[18] antibacterial,[19] antihypertensive,[20] antimalarial, antiviral, antiallergic, antibronchitic, analgesic, cardiotonic, herbicidal activities, and antitumor.[21]

In addition, dihydropyrano[3,2-*c*]chromene compounds are very beneficial structures in different areas of biology, pharmacology, and chemistry.[22] The common methods for the generation of pyrano [2,3-*d*] pyrimidine-2,4(1*H*,3*H*)-diones include the reaction of barbituric acid with arylidenemalononitriles under microwave irradiation[23] or standard hot conditions.[24] Many of mentioned organic rings demonstrate anticoagulant, anticancer, spasmolytic, antianaphylactic, and diuretic activity. Also, they can be utilized as cognitive booster, for controlling neurodegenerative diseases, such as Huntington's disease, Alzheimer's disease, AIDS-associated dementia, Parkinson's disease, amyotrophic lateral sclerosis, and Down's syndrome as well as for the therapy of myoclonus and schizophrenia.[25] Scheme 1 showed some biological examples of pyran and chromene derivatives as drugs.

Although lots of attempts have been made for the synthesis of pyran derivatives including anchored dysprosium and praseodymium complexes on $CoFe_2O_4$,[13] visible light irradiation promoted catalyst free and solvent free,[26] nano-CuO–Ag,[27] piperazine-1,4-diium dihydrogen phosphate,[28] imidazole-based bis-dicationic Brönsted acidic ionic liquids,[29] carboxy group functionalized imidazolium salts,[30] Ni^{2+} supported on hydroxyapatite-core-shell-γ-Fe_2O_3,[6] [EMIM][OH] ionic liquid,[31] and Fe_3O_4@APTES@isatin-SO_3H,[32] and the same attempts have been carried out for the synthesis of chromene such as CTMAB-bentonite,[33] Ni(II)-Schiff base/SBA-15,[34] Co_3O_4/NiO@GQDs@SO_3H,[35] $BF_3{\cdot}SiO_2$,[36] α-Fe_2O_3,[37] and CuO nanoparticles.[38] Previous reported methods introduced in literature have some drawbacks such as long reaction times, drastic conditions, poor recovery of expensive catalysts, complex synthetic pathways, and unsatisfactory yields. Thus, according to their significance from industrial, synthetic and pharmacological sectors introducing a novel, efficient, and eco-friendly protocol for the preparation of these heterocycle compounds have attracted significant interest.

On the other hand, magnetic nanoparticles (MNPs) have particularly drawn attention as their magnetic properties can greatly facilitate the application and separation of compounds.[39–42] Magnetic isolation is eco-friendly, quick, and more effective than centrifugation and filtration.[43–46] Among the various MNPs, Fe_3O_4 seems to be the most interesting magnetic substance for the catalyst support; however, Fe_3O_4 is quite chemically unstable. On the contrary, cobalt ferrite ($CoFe_2O_4$), which is a typical ferromagnetic oxide, has high thermal constancy, moderate magnetization, mechanical rigidity, and the significant chemical stability.[47] Among several spinel ferrites, cobalt ferrite ($CoFe_2O_4$) is especially well accepted due to using inexpensive commercially available materials, and as it is, easily prepared, being moisture insensitive, and readily separated from reaction mixture.[48,49] Also, they possess distinguished properties such as high chemical, mechanical, and thermal stability; high magnetism; large specific surface area; and moderate magnetization saturation. So extensive use of $CoFe_2O_4$ in various fields like biomedical, photocatalyst, photomagnetic drug delivery

SCHEME 1 Some biological activity of pyrimidine and chromene rings

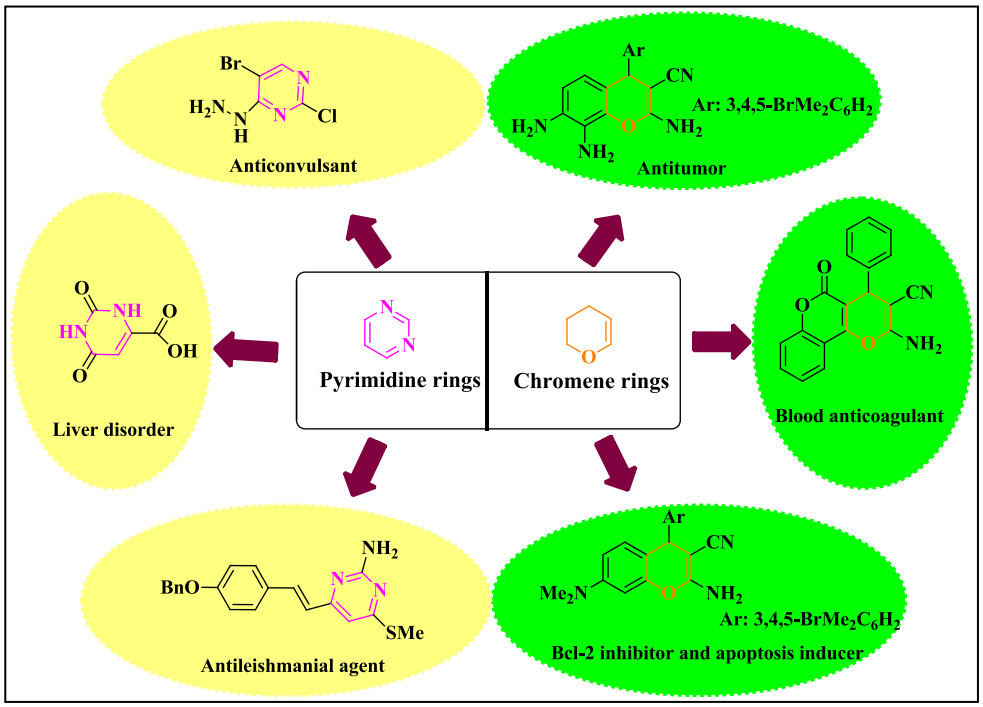

in the cancer therapy, and electronics have been reported.[50]

It should be mentioned that folic acid (FA) is a type of vitamin B complex. Folate receptors express at low levels in most normal cells. Moreover, FA is a small molecule that is soluble in water and possesses high stability.[51] It is worth noting, FA as enzymatic cofactor has significant effect in methyl-group transference reactions, and it is tied with a several biological functions.[52] In the current research, FA is used as green linker to facilitate anchoring metals on $CoFe_2O_4$. Scheme 2 illustrates the method for the preparation of $CoFe_2O_4$@FA-Er stepwise.

Encouraged by these attempts and intended to display the generality and performance of $CoFe_2O_4$@FA-Er as catalyst, we have used this new catalyst for the preparation of pyrano[2,3-*d*]pyrimidinone and dihydropyrano[3,2-*c*]chromenes from accessible starting compounds under moderate reaction conditions. Compared with other substrates, $CoFe_2O_4$@FA-Er nanoparticles have many advantages such as easy and efficient reusability, high loading capacity, short reaction time, low leaching, and easy isolation by magnetic field.

2 | EXPERIMENTAL

2.1 | Instruments and materials

All chemical and solvents were purchased from Sigma-Aldrich and Merck chemical companies and were applied without extra purification. The surface morphology and diameter of the $CoFe_2O_4$@FA-Er nanocatalyst was studied by field emission scanning electron microscopy (FE-SEM) analysis data, which was recorded by SEM-TESCAN MIRA3. Transmission electron microscopy (TEM) was carried out using a FEI CM200 field emission at accelerating voltage of 80 kV. The X-ray diffraction (XRD) was recorded on JEOL JSM-6100 microscope with (Cu Kα radiation, $\lambda = 1.54$ Å). The thermal gravimetric analysis (TGA) of nanocomposite was carried out on a Shimadzu analyzer DTG-60. Magnetic properties of the samples were identified using a vibrating sample magnetometer (VSM) at room temperature (MDKFD, University of Kashan, Iran). The amount of Er in the synthesized nanocatalyst was evaluated by inductively coupled plasma-optical emission spectrometry (ICP-OES). Fourier-transform infrared (FT-IR) spectra of all samples were recorded on Perkin Elmer Spectrum One instruments, using KBr pellets in the range of 400-4000 cm^{-1}. ^1H and ^{13}C nuclear magnetic resonance (NMR) spectra were measured on a Bruker 400-MHz spectrometer in DMSO with chemical shift (δ) given in ppm.

2.2 | Synthesis of $CoFe_2O_4$ nanocomposite

In a round-bottom flask (250 ml), a solution of $FeCl_3{\cdot}6H_2O$ (2.7 g, 10 mmol) and $CoCl_2{\cdot}6H_2O$

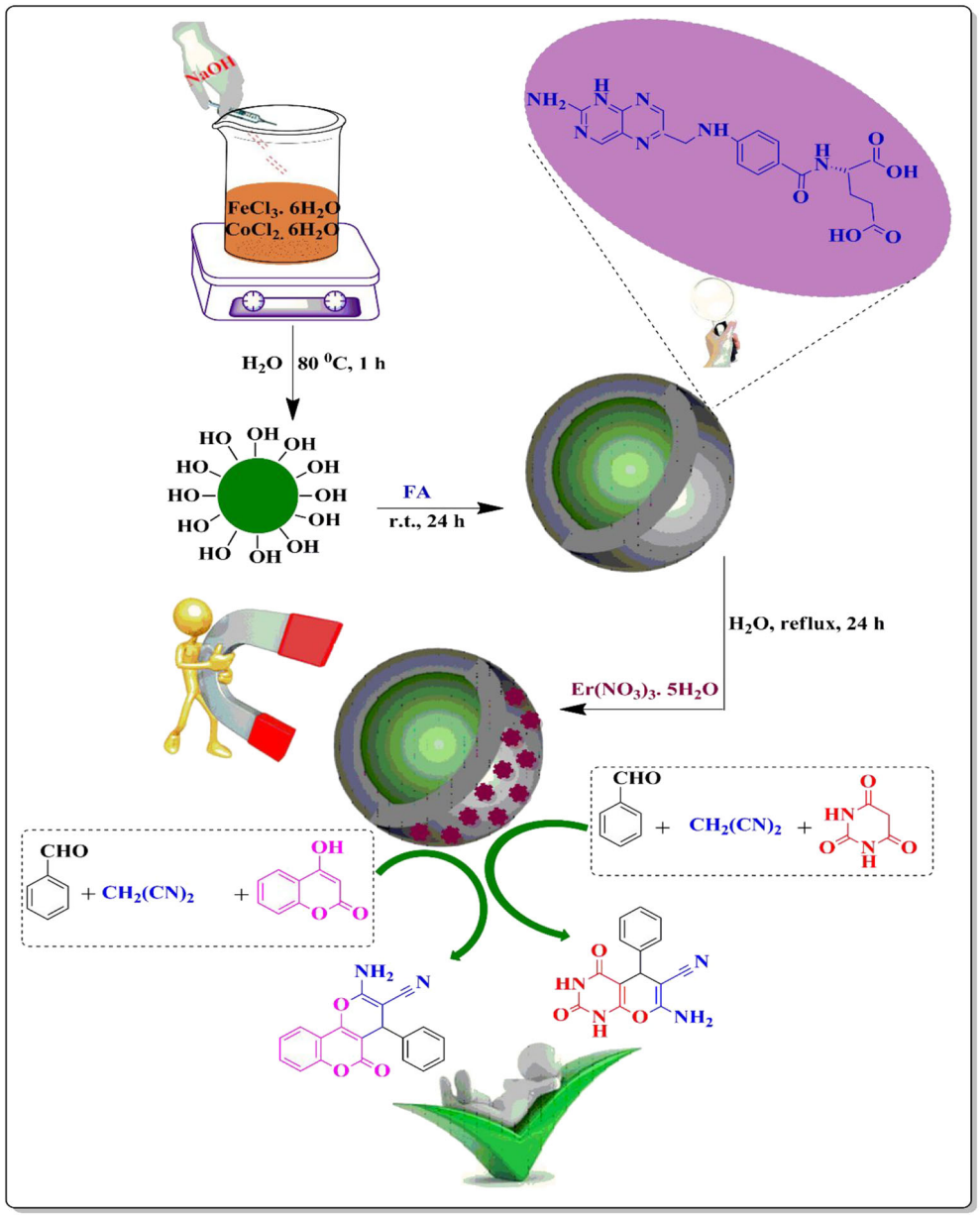

SCHEME 2 Synthetic approach to $CoFe_2O_4$@FA-Er magnetic nanoparticles (MNPs)

(1.189 g, 5 mmol) in distilled water (30 ml) was mixed and sonicated for 15 min. Next step, 25% aqueous sodium hydroxide 3 M was added dropwise along with stirring to form brown solid particles. When the reaction mixture reached pH = 11–12, the prepared $CoFe_2O_4$ nanostructure was isolated by an external magnet and was washed several times with ethanol and distilled water to eliminate any contaminants, and afterwards, it was dried at 60°C for 6 h in an oven.

2.3 | Synthesis of $CoFe_2O_4$@FA

Similarly, to produce $CoFe_2O_4$@FA, a solution of FA (1 g in 25-ml double distilled water) was added dropwise to suspensions of 2-g $CoFe_2O_4$ in 30-ml distilled water. Then, the reaction compound was stirred for 24 h at room temperature. Finally, the prepared nanocomposite was isolated using an external magnet, washed with double distilled water/ethanol multiple times, and dried in vacuum oven at 60°C.

2.4 | Synthesis of $CoFe_2O_4$@FA-Er nanocomposite

To expand the scope of the processes, we produced the $CoFe_2O_4$@FA-Er by blending sonicated $CoFe_2O_4$@FA (1 g) in 50 ml of double distilled water and a solution of 5-ml $Er(NO_3)_3{\cdot}5H_2O$ (0.886 g, 2 mmol) was added to the

mentioned mixture and was stirred under reflux for 24 h. Then, the achieved product was isolated using an external magnet and was washed with double distilled water/ethanol several times then dried in a vacuum oven at 60°C.

2.5 | A general method for the synthesis of pyrano[2,3-*d*]pyrimidinone

To a mixture of aromatic aldehyde (1 mmol), barbituric acid, and malononitrile (1 mmol), 30-mg $CoFe_2O_4$@FA-Er was added and heated at 100°C under solvent-free conditions or at 80°C under sonication in water as a green solvent for a suitable period of time as represented in Table 2. The progress of the reaction was controlled by TLC (*n*-hexane/EtOAc, 10:3). At the end of the reaction, 5-ml EtOAc was added, and the magnetic nanocatalyst was separated from the reaction vessel by an external magnet bar. The remained solid was separated with EtOAc (10 ml) and dried with anhydrous Na_2SO_4. After evaporation of EtOAc, the expected product was formed by recrystallization in hot EtOH. The desired crude product was identified by comparison of their physical data with those of known pyrano[2,3-*d*]pyrimidinone.

2.5.1 | 7-Amino-5-(4-methoxyphenyl)-2,4-dioxo-1,3,4,5-tetrahydro-2*H*-pyrano[2,3-*d*]pyrimidine-6-carbonitrile

Yellow powder, IR (KBr, cm^{-1}): 3322 (NH_2), 3281, 3140 (NH), 3065 (CH), 2218 (CN), 1746 (CO), 1666 (CC). ^{1}H NMR (400 MHz, DMSO-d_6): $\delta = 10.93$ (s, 1H, NH), 10.70 (s, 1H, NH), 7.16 (d, $J = 7.5$ Hz, 2H, Ar-H), 6.84–6.81 (m, 4H, Ar-H and NH_2), 4.18 (s, 1H, CH), 3.82 (s, 3H, OCH_3) ppm. ^{13}C NMR (100 MHz, DMSO-d_6): $\delta = 161.9$ (CO), 158.1 (C-14), 154.5 (CNH_2), 150.9 (CONH), 150.2 (CO), 130.3 (C-11), 129.5 (C-12), 123.6 (CN), 113.1 (C-13), 93.4 (C-5), 58.6 (C-9), 57.4 (CH_3), 53.4 (C-10) (Table 2, Entry 6).

2.5.2 | 7-Amino-5-(4-hydroxyphenyl)-2,4-dioxo-2,3,4,5-tetrahydro-1*H*-pyrano[2,3-*d*]pyrimidine-6-carbonitrile

Yellow powder, IR (KBr, cm^{-1}): 3450 (OH), 3258 (NH_2), 3126, 3088 (NH), 2295 (CH), 2235 (CN), 1734 (CO), 1670 (CO), 1557 (CC). ^{1}H NMR (400 MHz, DMSO-d_6): $\delta = 10.90$ (s, 1H, NH), 10.83 (s, 1H, NH), 6.93 (d, $J = 7.5$ Hz, 2H, Ar-H), 6.89 (s, 2H, NH_2), 6.57 (d, $J = 7.6$ Hz, 2H, Ar-H), 6.01 (s, 1H, OH), 4.33 (s, 1H, CH) ppm. ^{13}C NMR (100 MHz, DMSO-d_6): $\delta = 168.9$ (CO), 157.26 (C-14), 155.6 (CNH_2), 153.3 (CONH), 152.7 (CO), 129.29–129.1 (C-12 and C-16), 119.1 (CN), 116.2 (C-13), 97.3 (C-5), 58.6 (C-9), 54.9 (C-10) (Table 2, Entry 9).

2.5.3 | 7-Amino-5-(2,3-dichlorophenyl)-1,3-dimethyl-2,4-dioxo-2,3,4,5-tetrahydro-1*H*-pyrano[2,3-*d*]pyrimidine-6-carbonitrile

White solid, IR (KBr, cm^{-1}): 3410, 3319, 3196, 2932, 2197, 1712, 1695, 1642, 1486, 1387, 1233, 1180, 1048, 754. ^{1}H NMR (400 MHz, DMSO-d_6): $\delta = 3.09$ (s, 3H, NMe), 3.42 (s, 3H, NMe), 4.94 (s, 1H, CH), 7.26–7.43 (m, 5H, Ar-H and NH_2). ^{13}C NMR (100 MHz, DMSO-d_6): $\delta = 29.1$, 30.4, 58.6, 89.3, 121, 130.1, 130.5, 130.6, 132.2, 133.4, 151.6, 153.5, 159.6, 161.8 (Table 2, Entry 10).

2.5.4 | 7-Amino-5-(4-chloro-3-nitrophenyl)-1,3-dimethyl-2,4-dioxo-2,3,4,5-tetrahydro-1*H*-pyrano[2,3-*d*]pyrimidine-6-carbonitrile

White solid, IR (KBr, cm^{-1}): 3398, 3315, 3193, 2205, 1720, 1693, 1643, 1485, 1390, 1232, 1185, 1044, 972, 753, 504. ^{1}H NMR (400 MHz, DMSO-d_6): $\delta = 3.03$ (s, 3H, NMe), 3.41 (s, 3H, NMe), 4.52 (s, 1H, CH), 7.45–7.89 (m, 5H, NH_2 and Ar-H). ^{13}C NMR (100 MHz, DMSO-d_6): $\delta = 29.5$, 30.5, 37.8, 58.9, 88.6, 120.4, 125.1, 125.5, 132.5, 134.4, 146.8, 149.5, 151.8, 153.3, 159.7, 161.9 (Table 2, Entry 11).

2.5.5 | 7-Amino-5-(2-fluorophenyl)-1,3-dimethyl-2,4-dioxo-2,3,4,5-tetrahydro-1*H*-pyrano[2,3-*d*]pyrimidine-6-carbonitrile

White solid, IR (KBr, cm^{-1}): 3390, 3312, 3194, 2196, 1705, 1687, 1641, 1490, 1390, 1235, 1192, 1039, 969, 760, 572. ^{1}H NMR (400 MHz, DMSO-d_6): $\delta = 3.04$ (s, 3H, NMe), 3.39 (s, 3H, NMe), 4.59 (s, 1H, CH), 7.10–7.36 (m, 6H, Ar-H and NH_2). ^{13}C NMR (100 MHz, DMSO-d_6): $\delta = 29.2$, 30.7, 32, 58.7, 89.2, 116.7, 117, 120.4, 126.0, 130.4, 131.4, 132.2, 132.3, 151.5, 153, 159.5, 160.4, 161.9, 162.9 (Table 2, Entry 12).

2.6 | General method for the preparation of 3,4-dihydropyrano[*c*]chromene

To a mixture of aromatic aldehyde (1 mmol), malononitrile (1.2 mmol), and 4-hydroxycoumarin

(1 mmol), 40-mg $CoFe_2O_4$@FA-Er was added, and it was heated at 80°C under solvent-free conditions or at 80°C under sonication in water as a green solvent for a suitable period of time as shown in Table 3. The progress of the reaction was controlled by TLC (*n*-hexane/EtOAc, 10:4). After completion of the reaction, 5-ml EtOAc was added, and the magnetic nanocatalyst was isolated from the reaction vessel using an external magnet bar. The remained solid was separated with EtOAc (10 ml) and dried with anhydrous Na_2SO_4. After evaporation of EtOAc, the expected product was formed by recrystallization in hot EtOH. The desired crude product was identified by comparison of their physical data with those of known 3,4-dihydropyrano[*c*]chromene.

2.6.1 | 2-Amino-4-(4-methylphenyl)-3-cyano-5-oxo-4*H*,5*H*-pyrano[3,2-*c*] chromene

IR (KBr, cm^{-1}): 3390, 3310, 3188, 2190, 1702, 1670, 1616, 1375, 1050, 753. ^{1}H NMR (250 MHz, DMSO, ppm): $\delta = 2.60$ (s, 3H, CH_3), 4.38 (s, 1H, H-4), 7.14 (s, 2H, $J = 7.5$ Hz, HAr), 7.10 (s, 2H, $J = 7.5$ Hz, HAr), 7.43 (br s, 2H, NH_2), 7.50 (dd, 2H, $J = 7.5$, 4.5 Hz, HAr), 7.76 (t, 1H, $J = 7.5$ Hz, HAr), 7.90 (dd, 1H, $J = 7.5$, 1.25 Hz, HAr). ^{13}C NMR (100 MHz, DMSO-d_6): $\delta = 21.4$, 27.6, 29.2, 33.7, 36.1, 50.8, 60, 113.6, 120.6, 127.8, 129.6, 136.4, 142.7, 158.4, 163.1, 196.4 (Table 4, Entry 2).

2.6.2 | 2-Amino-4-(4-florophenyl)-3-cyano-5-oxo-4*H*,5*H*-pyrano[3,2-*c*] chromene

White solid, IR (KBr, cm^{-1}): 3374, 3282, 3188, 2191, 1710, 1678, 1609, 1501, 1373, 1508, 1603, 1380, 1222, 1064, 846, 755. ^{1}H NMR (250 MHz, DMSO, ppm): $\delta = 4.4$ (s, 1H, H-4), 7.21 (d, 2H, $J = 8.5$ Hz, HAr), 7.32 (t, 2H, $J = 7.25$ Hz, HAr), 7.35 (br s, 2H, NH_2), 7.46 (d, 1H, $J = 7.25$ Hz, HAr), 7.48 (1H, t, $J = 7.5$ Hz, HAr), 7.66 (1H, dt, $J = 5$, 1.5 Hz, HAr), 7.97 (dd, 1H, $J = 7.7$, 1.25 Hz, HAr). ^{13}C NMR (100 MHz, DMSO-d_6): $\delta = 27.3$, 27.7, 32.1, 38.4, 40.3, 50.1, 58.5, 113.1, 114, 120.2, 129, 142, 156, 196.2 (Table 4, Entry 7).

2.6.3 | 2-Amino-4-(2,4-dimethoxyphenyl)-3-cyano-5-oxo-4*H*,5*H*-pyrano[3,2-*c*] chromene

White solid, IR (KBr, cm^{-1}): 3549, 3390, 3339, 3209, 2189, 1716, 1673, 1604, 1378, 1300, 1199, 1053, 758. ^{1}H NMR

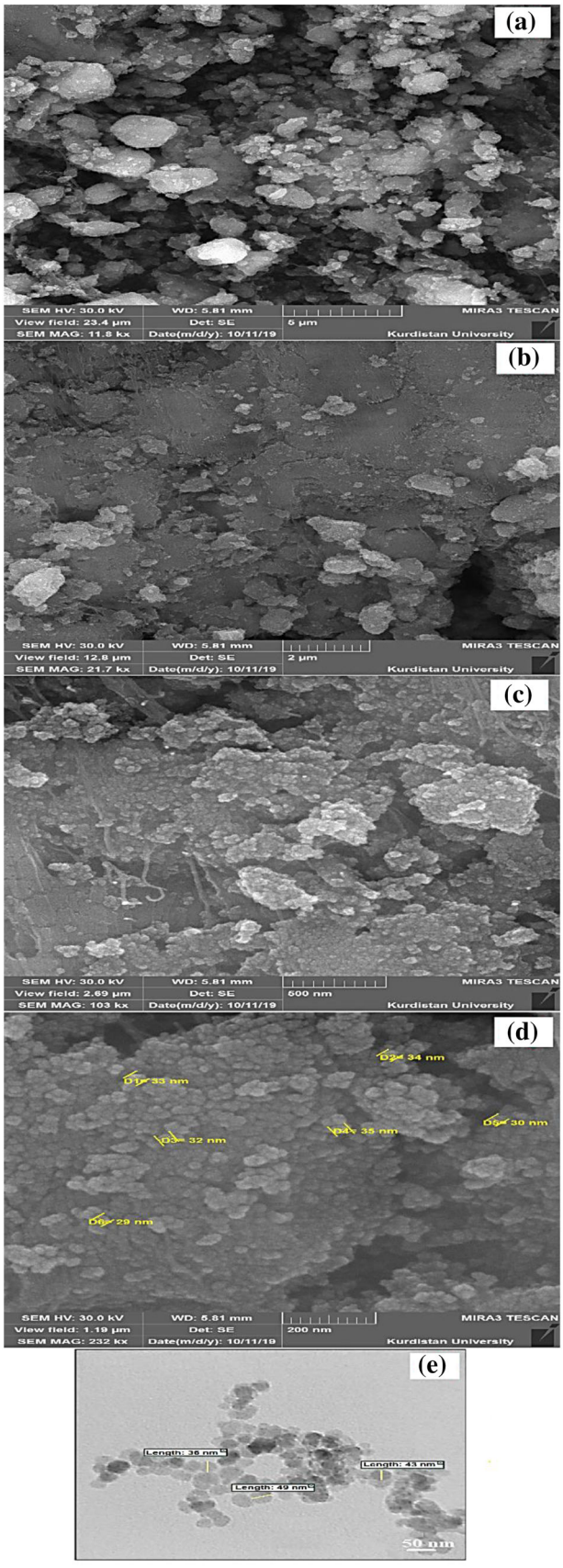

FIGURE 1 Field emission scanning electron microscopy (FE-SEM) images of $CoFe_2O_4$@FA-Er nanocatalyst at (a) 5 µm, (b) 2 µm, (c) 500 nm, and (d) 200 nm magnifications and (e) transmission electron microscopy (TEM) image of $CoFe_2O_4$@FA-Er nanocatalyst

(250 MHz, DMSO, ppm): $\delta = 3.69$ (s, 3H, OCH_3), 3.76 (s, 3H, OCH_3), 4.58 (s, 1H, H-4), 6.48 (dd, 1H, $J = 7.5$, 2.25 Hz, HAr), 6.51 (d, 1H, $J = 7.5$ Hz, HAr), 6.98 (d, 1H, $J = 8.5$ Hz, HAr), 7.19 (br s, 2H, NH_2), 7.49 (dd, 2H, $J = 7.5$, 1.5 Hz, HAr), 7.67 (dt, 1H, $J = 7.5$, 1.25 Hz, HAr), 7.95 (dd, 1H, $J = 7.5$, 1.5 Hz, HAr) (Table 4, Entry 10).

2.6.4 | 2-Amino-4-(2,4-dichlorophenyl)-3-cyano-5-oxo-4*H*,5*H*-pyrano[3,2-*c*] chromene

White solid, IR (KBr, cm^{-1}): 3465, 3296, 3159, 3071, 2200, 1720, 1669, 1590, 1377, 1062, 760. ^1H NMR (250 MHz, DMSO, ppm): $\delta = 5.03$ (s, 1H, H-4), 7.39 (dd, 1H, $J = 8.5$, 2 Hz, HAr), 7.41 (d, 1H, $J = 8.25$ Hz, HAr), 7.39 (br s, 2H, NH_2), 7.45 (d, 1H, $J = 8.3$ Hz, HAr), 7. 57 (t, 1H, $J = 8.25$ Hz, HAr), 7.62 (d, 1H, $J = 7.75$ Hz, HAr), 7.76 (dt, 1H, $J = 7.5$, 1.5 Hz, HAr), 7.93 (dd, 1H, $J = 7.0$, 1.5 Hz, HAr) (Table 4, Entry 11).

3 | RESULTS AND DISCUSSION

3.1 | Catalyst preparation

$CoFe_2O_4$@FA-Er was generally prepared in a three-step process. First, we synthesized $CoFe_2O_4$ by coprecipitation of Co^{2+} and Fe^{2+} ions. At the second step, FA ligand was coated over the surface of magnetic core to achieve functionalized MNPs. Finally, $CoFe_2O_4$@FA-Er nanocatalyst was gained by stable interaction of Er with O and N atom of FA ligand (Scheme 2). The

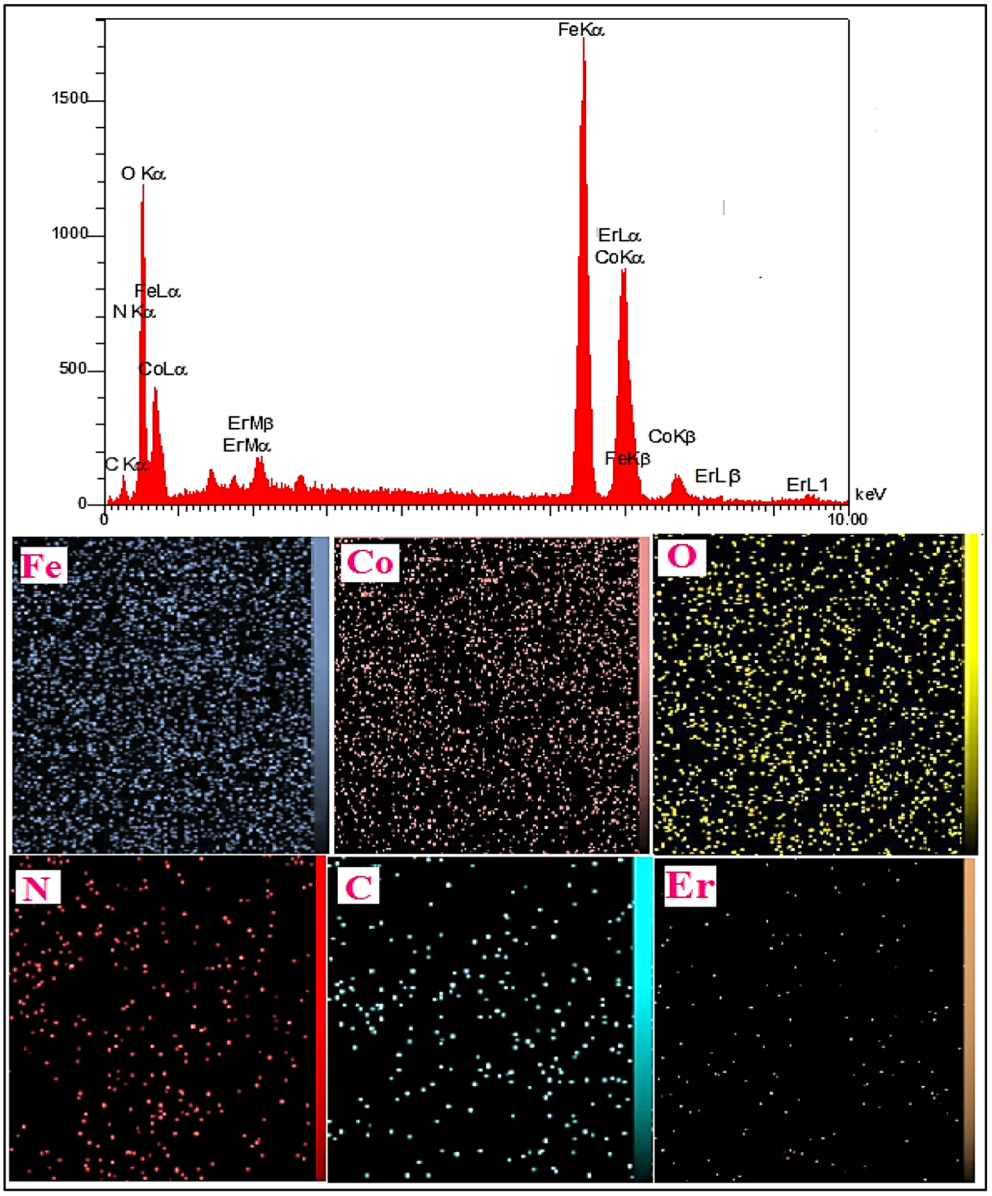

FIGURE 2 Energy-dispersive X-ray spectroscopy (EDX) and X-ray atomic mapping images of $CoFe_2O_4$@FA-Er magnetic nanoparticles (MNPs)

heterogeneous catalyst was synthesized successfully and was confirmed by several characterization methods such as FE-SEM, TEM, energy-dispersive X-ray spectroscopy (EDX), X-ray atomic mapping, TGA, XRD, VSM, ICP-OES, and FT-IR spectroscopy.

3.2 | Catalyst characterization

3.2.1 | FE-SEM and TEM studies

To illustrate the external texture and surface morphology of the obtained nanocatalyst, FE-SEM imaging in various magnification was performed (Figure 1).

The SEM analysis shows particles, homogeneous shape, and size, and the partly agglomerated form is due to high concentration during sampling. Therefore, specific surface area was presented for anchoring of Er over the whole matrix. It should be mentioned that the nanoparticles size was estimated to be in the range of 30–35 nm. Also, the TEM confirm the core-shell structure, and as displayed in Figure 1e, the size of the nanocatalyst is around 50 nm.

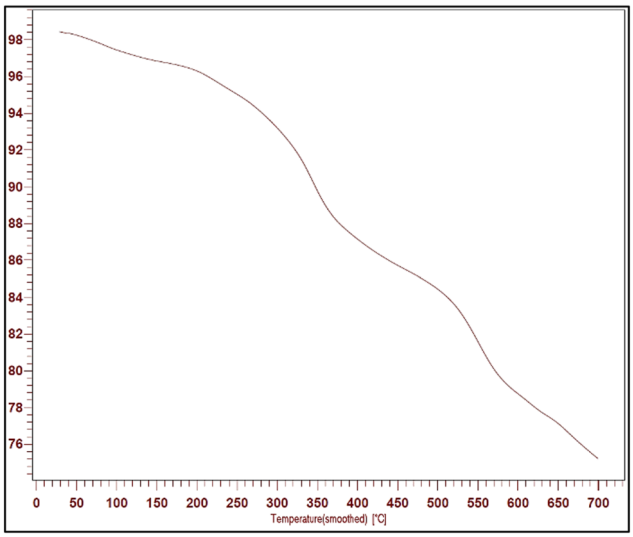

FIGURE 3 Thermal gravimetric analysis (TGA) profile of $CoFe_2O_4$@FA-Er magnetic nanoparticles (MNPs)

3.2.2 | EDX and X-ray atomic map studies

The energy-dispersive X-ray spectroscopy (EDX) and X-ray atomic mapping were performed to verify the presence of elements (Figure 2). Investigation of the results indicates the uniform dispersion of Er as an active site immobilized over FA by the side of the other core elements in the nanocatalyst.

3.2.3 | TGA studies

The thermal stability of $CoFe_2O_4$@FA-Er was reported using TGA (Figure 3). The TGA pattern shows an initial small weight loss below 200°C, and the next weight loss at about 250°C to 650°C is belonging to the disintegration of the grafted organic layers on the surface of $CoFe_2O_4$ magnetic nanocomposite.[53] The TGA profile demonstrates that the nanocatalyst has a sensible stability up to 200°C. These analyses entirely displayed that the nanocatalyst can be utilized successfully in heterogeneous systems around mentioned temperature.

3.2.4 | XRD studies

In order to illustrate the textural and phase behavior of introduced $CoFe_2O_4$@FA-Er MNPs, the powder XRD was performed (Figure 4). The XRD pattern of $CoFe_2O_4$ MNPs has been characterized by the peak status of 2θ values which is certainly certified (standard JCPDS values Card No. 22-1086). The crystalline spinel structures of $CoFe_2O_4$. The peak position of $CoFe_2O_4$@FA-Er

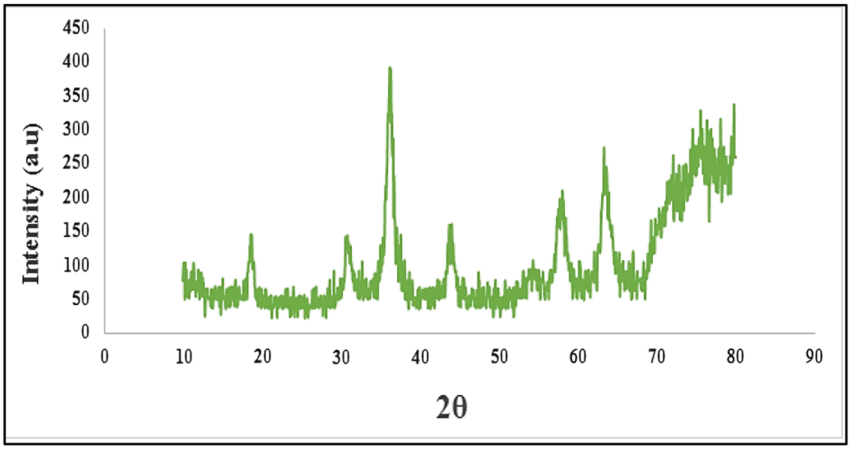

FIGURE 4 X-ray diffraction (XRD) pattern of $CoFe_2O_4$@FA-Er magnetic nanoparticles (MNPs)

at $2\theta = 19.61$, 31.08, 36.05, 43.32, 58.54, 65.70, and 74.81 were assigned to (1 1 1), (2 2 0), (3 1 1), (4 0 0), (4 2 2), (5 1 1), and (4 4 0) planes.[54] However, because of low concentration, the peaks related to Er phase could not be distinguished. Also, the crystalline size of the prepared nanocatalyst was calculated to be nearly 35 nm, as measured using the Debye–Scherrer equation.

3.2.5 | VSM studies

To compare magnetic property of bare $CoFe_2O_4$ with $CoFe_2O_4$@FA-Er nanoparticles, VSM technique was used (Figure 5). As shown, the saturation magnetization value (Ms) of the bare $CoFe_2O_4$ is 74.4 emu/g whereas after coating of NPs, the Ms value of $CoFe_2O_4$@FA-Er nanoparticles was found to be 36.2 emu/g. It is clear that the magnetic character for $CoFe_2O_4$ nanoparticles is more preferable than that of modified core which is related to the loading of organic layers and metal complexes on $CoFe_2O_4$ nanoparticles. Despite the decline in magnetic character of $CoFe_2O_4$@FA-Er, it is sensible enough to be quickly isolated from the reaction media by inducing an external magnetic field.

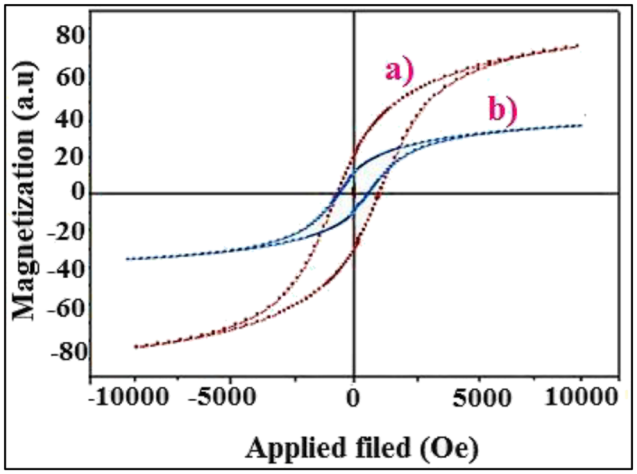

FIGURE 5 Vibrating sample magnetometer (VSM) curves of $CoFe_2O_4$@FA-Er magnetic nanoparticles (MNPs)

3.2.6 | ICP-OES studies

The exact amount of Er anchored on the surface of modified $CoFe_2O_4$ was measured to be 0.49 mmol/g by the aid of the ICP atomic emission spectroscopy method.

3.2.7 | FT-IR studies

Figure 6 exhibits FT-IR spectrum of synthesized nanoparticles. Spectrum of the $CoFe_2O_4$ (Figure 6a) obviously displays absorption bands at about 587 and 3461 cm^{-1}, which are indication of the existence of hydroxyl functional group (O–H) and metal–oxygen bond, respectively.[55,56] Also, FT-IR spectrum of bare FA is presented in Figure 6b. Its FT-IR spectrum illustrates obvious peaks at 3320–3550 cm^{-1} range, which belong to –NH and –OH bonds. Moreover, distinct peaks at

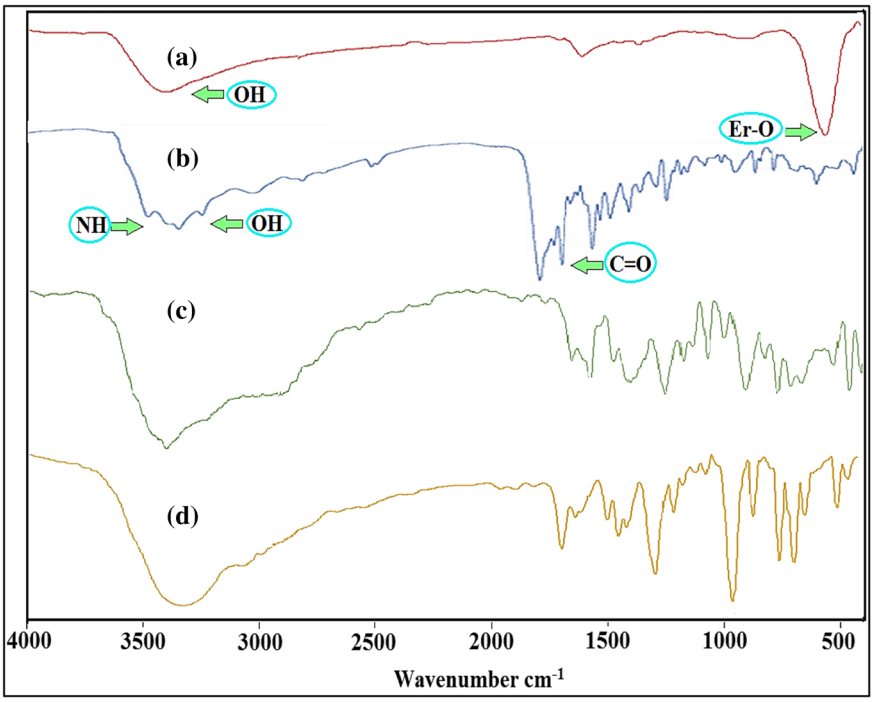

FIGURE 6 Fourier-transform infrared (FT-IR) spectra of (a) $CoFe_2O_4$, (b) FA, (c) $CoFe_2O_4$@FA, and (d) $CoFe_2O_4$@FA-Er magnetic nanoparticles (MNPs)

TABLE 1 Optimization experiments for a one-pot synthesis of the model reaction

Entry	Catalyst (mg)	Solvent	Reaction condition	Time (min)	Yield (%)
1	30	H_2O	Reflux	45	89
2	30	EtOH	Reflux	60	84
3	30	CH_3CN	Reflux	98	35
4	30	CH_2Cl_2	Reflux	98	32
5	30	EtOAc	Reflux	99	50
6	$CoFe_2O_4$	H_2O	Reflux	240	Trace
7	30	Solvent free	rt	100	75
8	30	Solvent free	80°C	30	91
9	**30**	**Solvent free**	**100°C**	**20**	**96**
10	25	Solvent free	100°C	35	94
11	$CoFe_2O_4$	H_2O	Sonication/rt	240	Trace
12	10	H_2O	Sonication/80°C	18	72
13	25	H_2O	Sonication/80°C	14	90
14	**30**	**H_2O**	**Sonication/80°C**	**10**	**92**

Note: Reaction conditions: bezaldehyde (1 mmol), barbituric acid (1 mmol), malononitrile (1 mmol), $CoFe_2O_4$@FA-Er catalyst under solvent-free conditions. The best results in performing the reaction are shown in bold.

1693–1705 cm^{-1} are observed for carboxylic acid groups.[57] Absorption peaks related to the loading of FA on the surface of the introduced $CoFe_2O_4$ nanoparticles are illustrated in Figure 6c. FT-IR spectra of the $CoFe_2O_4$@FA and $CoFe_2O_4$@FA-Er (Figure 6b,c) are similar and correspond to the patterns of $CoFe_2O_4$ and FA which shows that the main core is remained unchanged after immobilization of its surface and successful transfer to final nanostructure. It is worth noting that the little discrepancy between 2b and 2c is related to shift of Er metal to the internal scaffold.

3.3 | The catalytic activity

Due to confirmed ability of $CoFe_2O_4$@FA-Er as an efficient and mild magnetic nanocatalyst, the synthesized MNPs were used for the synthesis of pyrano[2,3-*d*] pyrimidinone. First, to gain the optimized reaction conditions, the reactions of barbituric acid, malononitrile, and benzaldehyde were selected as a model reaction. The appropriate conditions for the mentioned reaction were tested with different solvents such H_2O, EtOH, CH_3CN, CH_2Cl_2, and EtOAc in several temperatures in the presence of $CoFe_2O_4$@FA-Er as nanocatalyst. The results indicated when the reaction proceeds in solvent-free conditions and the favorable product was afforded in very short reaction time and excellent yield (96%). By increasing the reaction temperature to 100°C, the end time of reaction reduced to 15 min, so the optimized reaction conditions were gained (Table 1, Entry 9). Also, this three-component reaction was performed under the reflux condition in protic solvent including H_2O and EtOH and obtained the desired product in 90% yield (Table 1, Entries 1 and 6). Therewith, CH_3CN, CH_2Cl_2, and EtOAc as aprotic solvents generated the product in longer reaction times and lower yields (Table 1, Entries 3–5). Then, the optimized value of synthesized MNPs at 100°C under the solvent-free conditions was examined, and the best outcomes were generated in the presence of 30 mg of $CoFe_2O_4$@FA-Er. The efficacy of temperature was also investigated by proceeding the model reaction under the solvent-free condition and 30 mg of catalyst at room temperature, 80°C, and 100°C. By increasing the reaction temperature, the yield was increased (Table 1, Entry 9). Furthermore, the mentioned three-component reaction was tested without the $CoFe_2O_4$@FA-Er, and a negligible amount of the corresponding product was generated after 4 h (Table 1, Entry 6).

Then, in order to study the capability of sonication for fast progress of the considered reactions, the model reaction was tested in H_2O under the sonication at 80°C and in the presence of different amounts of nanocatalyst. As showed in Table 1, the best result was gained using 30 mg of $CoFe_2O_4$@FA-Er within 10 min, and the H_2O was the best solvent of choice. In order to justify the generality of the optimized condition and substrate scope of the introduced protocol, several aromatic aldehyde derivatives were used bearing electron-withdrawing

and electron-donating groups in the presence of $CoFe_2O_4$@FA-Er nanocatalyst and under optimized conditions. The results of generated desired products are summarized in Table 2. The outcomes indicated that the products were formed in excellent yields and short time. All products were known and characterized by melting points. In addition, the spectral and analytical (IR, ^1H, and ^{13}C, NMR) data of products were studied to determine the structures and were compared directly with authentic samples.

TABLE 2 Condensation of pyrano[2,3-*d*]pyrimidinone compounds in the presence of $CoFe_2O_4$@FA-Er

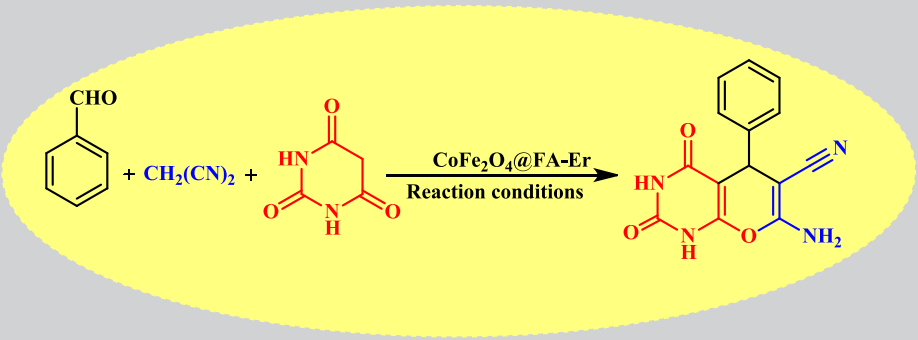

Entry	Aldehyde	Product	100°C/solvent free Time (min)	100°C/solvent free Yield (%)	Sonication/ H_2O/80°C Time (min)	Sonication/ H_2O/80°C Yield (%)	M.p. °C Found/ Reported
1	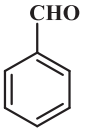	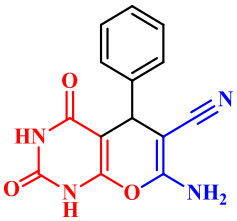	20	96	10	92	240–243 (260–262)[58]
2	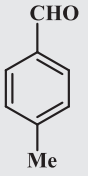	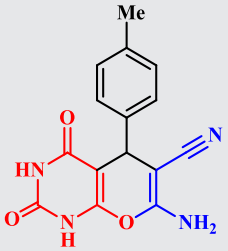	30	91	15	90	223–225 (225)[59]
3	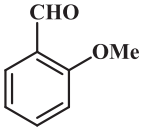	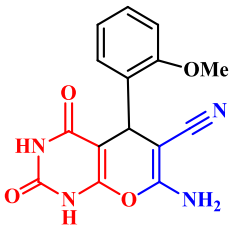	25	90	12	89	300 (301–302)[59]

(Continues)

TABLE 2 (Continued)

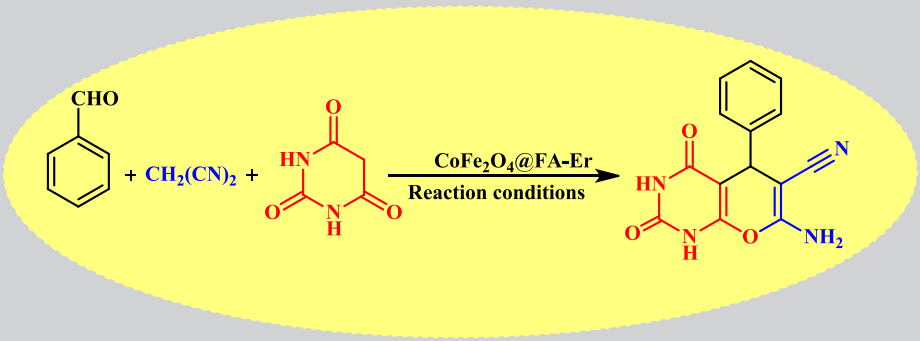

Entry	Aldehyde	Product	100°C/solvent free Time (min)	100°C/solvent free Yield (%)	Sonication/ H2O/80°C Time (min)	Sonication/ H2O/80°C Yield (%)	M.p. °C Found/ Reported
4	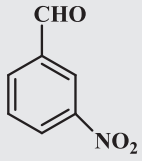	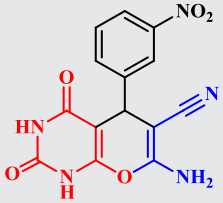	20	95	8	93	254–255 (255–257)[59]
5	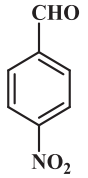	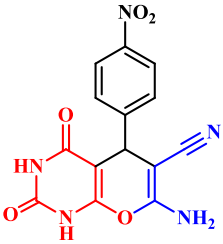	15	96	10	94	230 (227–229)[23]
6	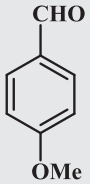	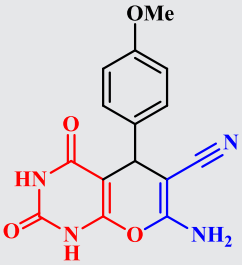	25	93	12	90	280–283 (280)[59]
7	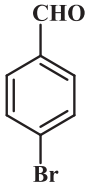	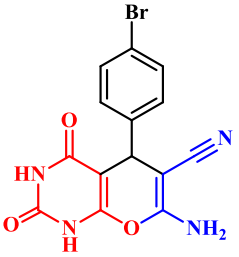	25	94	10	90	216–218 (217–219)[60]

TABLE 2 (Continued)

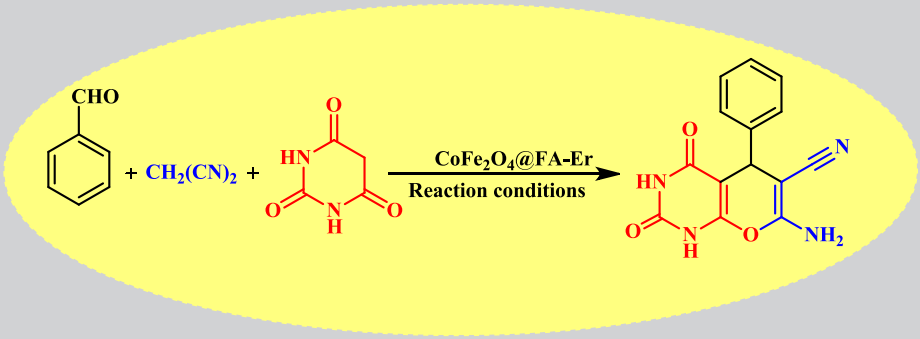

Entry	Aldehyde	Product	100°C/solvent free Time (min)	100°C/solvent free Yield (%)	Sonication/ H2O/80°C Time (min)	Sonication/ H2O/80°C Yield (%)	M.p. °C Found/ Reported
8	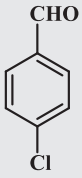	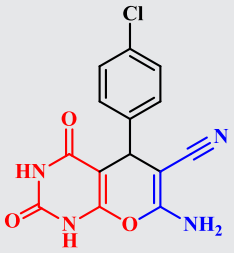	25	93	12	89	231–233 (229–230)[23]
9	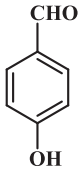	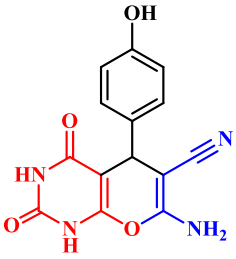	30	90	14	88	289–292 (289)[59]
10	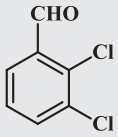	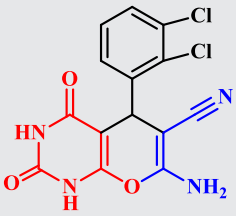	30	89	14	87	210–213 (211–212)[61]
11	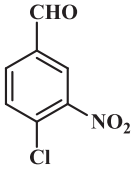	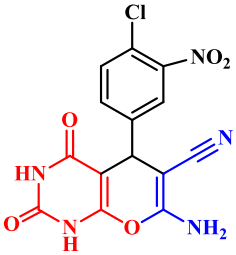	29	87	15	87	208–211 (209–210)[61]

(Continues)

TABLE 2 (Continued)

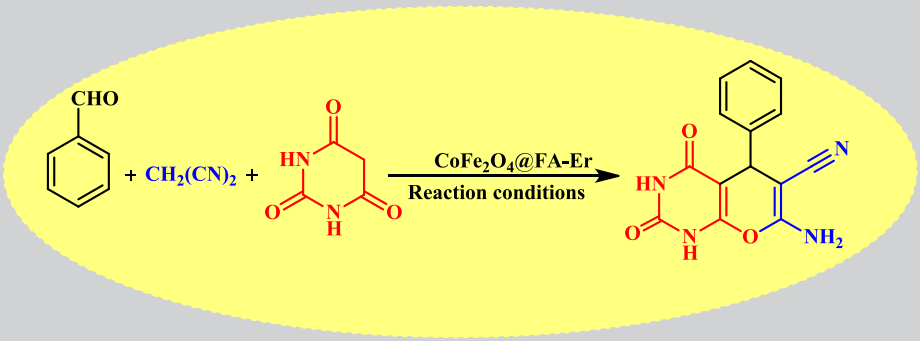

Entry	Aldehyde	Product	100°C/solvent free Time (min)	100°C/solvent free Yield (%)	Sonication/ H_2O/80°C Time (min)	Sonication/ H_2O/80°C Yield (%)	M.p. °C Found/ Reported
12	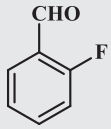	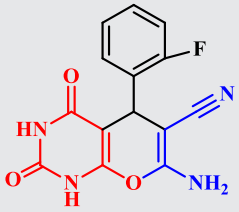	30	88	13	88	238–240 (238–239)[61]

Note: Reaction conditions: bezaldehyde (1 mmol), barbituric acid (1 mmol), malononitrile (1 mmol), under solvent free, $CoFe_2O_4$@FA-Er (30 mg) or H_2O (5 ml, sonication [28 kHz]).

TABLE 3 Condensation of a one-pot synthesis of the model reaction

Entry	Catalyst (mg)	Solvent	Reaction condition	Time (min)	Yield (%)
1	40	EtOH	Reflux	65	70
2	40	CH_2Cl_2	Reflux	120	35
3	40	CH_3CN	Reflux	100	40
4	40	EtOAc	Reflux	120	66
5	$CoFe_2O_4$	H_2O	80°C	240	Trace
6	40	H_2O	Reflux	60	82
7	40	Solvent free	60°C	45	89
8	**40**	**Solvent free**	**80°C**	**25**	**94**
9	35	Solvent free	80°C	35	91
10	30	Solvent free	80°C	45	87
11	$CoFe_2O_4$	H_2O	Sonication/rt	240	Trace
12	20	H_2O	Sonication/80°C	25	74
13	30	H_2O	Sonication/80°C	20	83
14	**40**	**H_2O**	**Sonication/80°C**	**14**	**91**

Note: Reaction conditions: bezaldehyde (1 mmol), 4-hydroxycoumarin (1 mmol), malononitrile (1.2 mmol), $CoFe_2O_4$@FA-Er catalyst under solvent-free conditions. The best results in performing the reaction are shown in bold.

TABLE 4 Synthesis of amino-4-aryl-3-cyano-5-oxo-4*H*,5*H*-pyrano[3,2-*c*]chromenes compounds in the presence of $CoFe_2O_4$@FA-Er

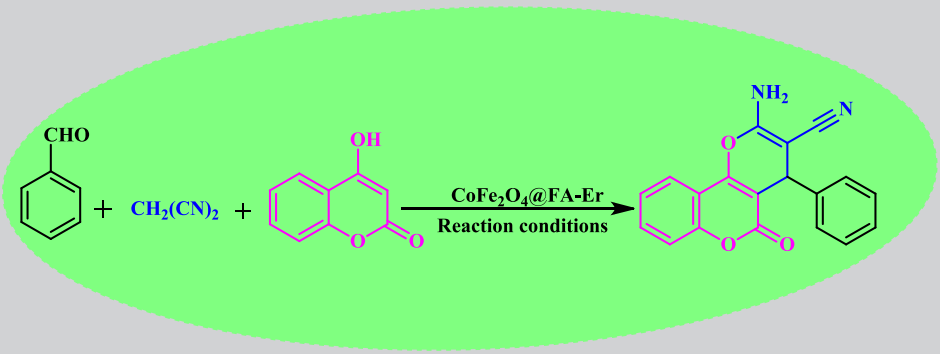

Entry	Aldehyde	Product	Solvent free/80°C		Sonication/ H_2O/80°C		M.p. °C Found/ Reported
			Time (min)	Yield (%)	Time (min)	Yield (%)	
1	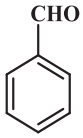	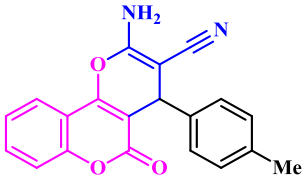	30	94	14	91	237–238 (236–239)[62]
2	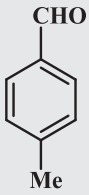	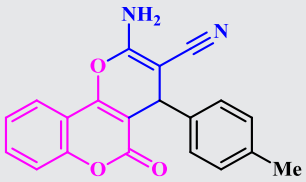	36	85	14	84	212–215 (214–216)[63]
3	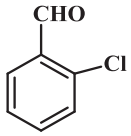	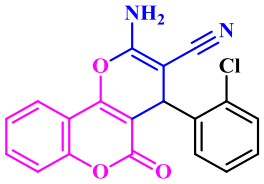	30	91	14	91	212–214 (212–213)[64]
4	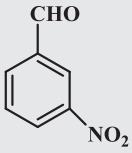	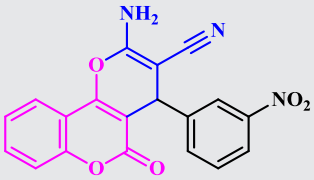	32	90	12	92	207–209 (210)[65]
5	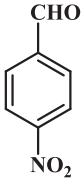	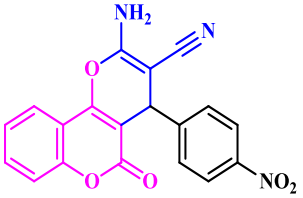	26	96	12	96	181–183 (180–182)[65]

(Continues)

TABLE 4 (Continued)

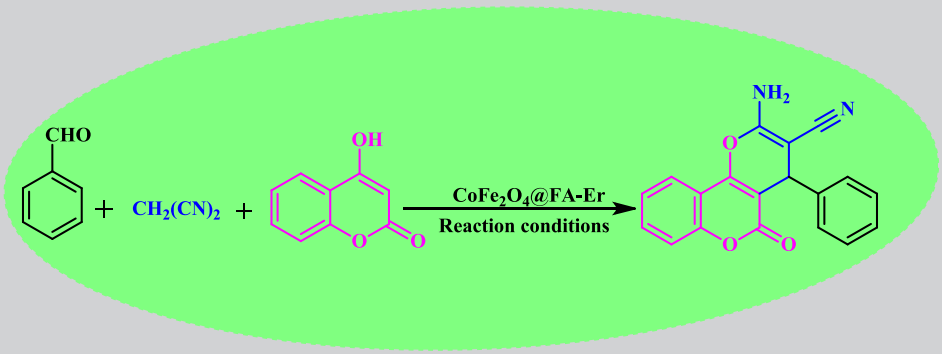

Entry	Aldehyde	Product	Solvent free/80°C Time (min)	Solvent free/80°C Yield (%)	Sonication/ H_2O/80°C Time (min)	Sonication/ H_2O/80°C Yield (%)	M.p. °C Found/ Reported
6	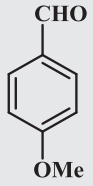	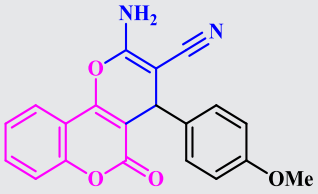	30	87	14	86	200–203 (198–202)[63]
7	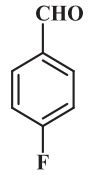	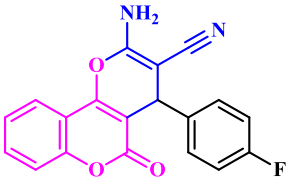	24	92	14	92	188–191 (190–192)[63]
8	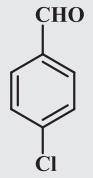	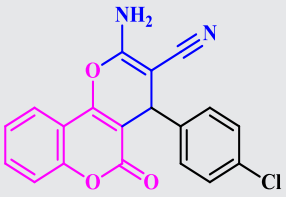	26	93	12	92	266–267 (265–267)[66]
9	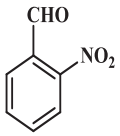	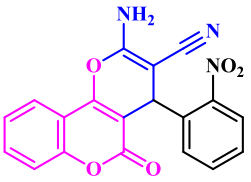	32	90	11	88	237–240 (238–239)[67]
10	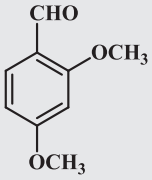	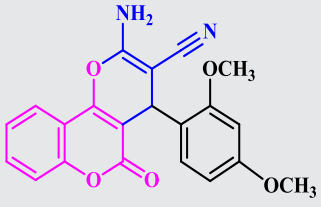	33	89	14	88	235–237 (236–238)[68]

TABLE 4 (Continued)

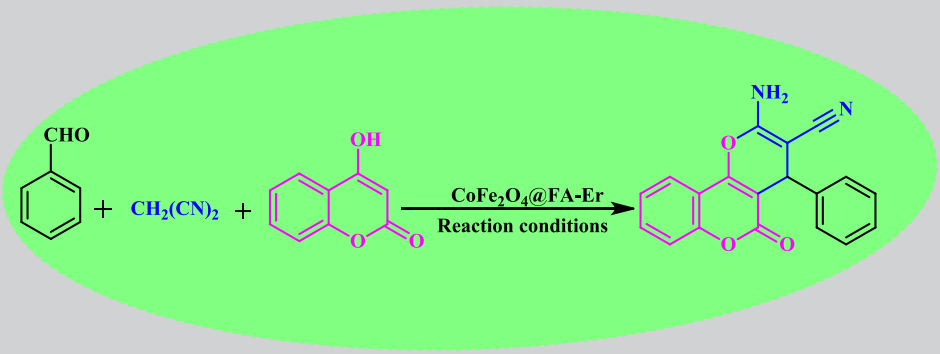

Entry	Aldehyde	Product	Solvent free/80°C Time (min)	Solvent free/80°C Yield (%)	Sonication/ H_2O/80°C Time (min)	Sonication/ H_2O/80°C Yield (%)	M.p. °C Found/ Reported
11	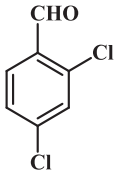	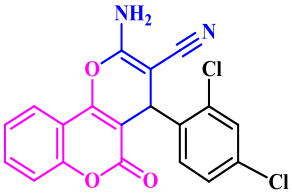	32	90	12	89	257–259 (256–257)[69]

Note: Reaction conditions: bezaldehyde (1 mmol), 4-hydroxycoumarin (1 mmol), malononitrile (1.2 mmol), under solvent free, $CoFe_2O_4$@FA-Er (40 mg) or water (5 ml, sonication [28 kHz]).

Next, to investigate another usage of nanocatalyst toward the formation of dihydropyrano[3,2-*c*] chromene, we displaced the barbituric acid with 4-hydroxycoumarin. For this purpose, malononitrile, dihydropyrano[3,2-*c*]chromene, and benzaldehyde were selected as a model reaction. Then, the efficacy of diverse solvents such as H_2O, EtOH, EtOAc, CH_2Cl_2, and CH_3CN were checked when the model reaction was proceeding in the presence of 40 mg of $CoFe_2O_4$@FA-Er conditions at different temperatures. The results are exhibited in Table 3. The best result in terms of the yield (94%) and the reaction time (25 min) was gained when the reaction accomplished at 80°C under the solvent-free condition (Table 3, Entry 8). Moreover, the model reaction was examined in the presence of 40-mg nanocatalyst at 60°C, and the desired product was obtained in lower yield and longer reaction time (Table 3, Entries 7). Also, it was confirmed that in the absence of nanocatalyst, only a negligible amount of the corresponding product was formed even after more than 4 h of heating (Table 3, Entry 5). The outcomes definitely indicated the catalyst efficiency in this condensation, and it showed that without $CoFe_2O_4$@FA-Er, even after higher reaction time, the reaction did not carry on.

In line with showing the generality of this approach, the obtained optimum conditions were used to synthesize a different derivative of aromatic aldehyde performed either electron-withdrawing or electron-donating groups in the different positions (*ortho*, *meta*, and *para*). The outcomes are illustrated in Table 4. It was found that the electron-withdrawing groups generated products in excellent yields not only under the sonication but also at 80°C under solvent-free condition. All products were known and characterized by melting points. In addition, the spectral and analytical (IR, ^1H, and ^{13}C, NMR) data of products were studied to determine the structures and were compared directly with authentic samples.

As can be found from Tables 2 and 4, the introduced catalyst successfully accelerated both pyrano[2,3-*d*] pyrimidinone and dihydropyrano[3,2-*c*]chromenes, and the favorable products were formed in high to excellent yields and short times.

To display the efficiency of the of $CoFe_2O_4$@FA-Er for the preparation of pyrano[2,3-*d*]pyrimidinone (Table 3, Entries 1–5) and dihydropyrano[3,2-*c*]chromenes condensation (Table 4, Entries 6–10), a comparison of different formerly reported procedures with current work is exhibited in Table 5. Investigation of the results illustrated

TABLE 5 Comparison the efficacy of $CoFe_2O_4$@FA-Er catalyst with some diverse catalysts in the preparation of pyrano[2,3-*d*] pyrimidinone (Entries 1–7) and dihydropyrano[3,2-*c*]chromenes condensation (Entries 8–15)

Entry	Catalyst	Condition	Time (min)	Yield (%)	Ref.
1	$CoFe_2O_4$@Glutamin-Pr (40 mg)	H_2O/rt/UV	15	95	Daraie et al.[13]
2	$CoFe_2O_4$@Glutamin-Dy (40 mg)	H_2O/rt/UV	15	92	Daraie et al.[13]
3	γ-Fe_2O_3@SiO_2@[Bis APTES]Cl_2-NPs (10 mg)	H_2O/EtOH (2:1)/80°C	12	85	Karimi-Chayjani et al.[70]
4	[H_2-Bisim][HSO_4]$_2$ (6.2 mol%)	H_2O/reflux	25	70	Daneshvar et al.[29]
5	ZnO@CuO (30 mg)	H_2O/reflux	12	91	Heravi et al.[59]
6	$CoFe_2O_4$@FA-Er (30 mg)	H_2O/100°C	15	96	This work
7	$CoFe_2O_4$@FA-Er (30 mg)	Sonication/H_2O/80°C	10	92	This work
8	Ni(II)-Schiff base/SBA-15 (50 mg)	H_2O/70°C	10–15	95	Pesyan et al.[34]
9	Co_3O_4/NiO@GQDs@SO_3H nanocomposite (4 mg)	EtOH (US: 40 W)	10	94	Shahbazi-Alavi et al.[35]
10	BF_3·SiO_2 (60 mg)	50°C	15–25	90	Akbari[36]
11	α-Fe_2O_3 (10 wt%)	EtOH/rt	30	93	Nagabhushana et al.[37]
12	CuO nanoparticles (15 mol%)	H_2O/100°C	6	93	Mehrabi and Kazemi-Mireki[38]
13	Nano-zinc oxide (10 mol %)	Reflux	90	49	Wang et al.[71]
14	$CoFe_2O_4$@FA-Er (40 mg)	H_2O/100°C	25	94	This work
15	$CoFe_2O_4$@FA-Er (40 mg)	Sonication/H_2O/80°C	14	91	This work

that $CoFe_2O_4$@FA-Er is more preferable to some former procedures in terms of reaction times, yields, the avoidance of toxic materials, the amount of the reagent, organic volatile solvents, and the simple isolation of the catalyst.

A possible mechanism for the preparation of pyrano[2,3-*d*]pyrimidinone is presented in Scheme 3. According to this mechanism, upon initial condensation of aldehyde with malononitrile, the intermediate (1) is formed under the catalytic effect of $CoFe_2O_4$@FA-Er MNPs.

Next, by nucleophilic addition of barbituric acid, the intermediate (1) joined successively by intramolecular cyclization to the intermediate (2), and rearranged to generate the desired product. An analogous mechanism may take place for the of dihydropyrano[3,2-*c*]chromene derivatives formation.

3.4 | Recycling $CoFe_2O_4$@FA-Er

Given the fact that today the recycling and reusing the catalyst are the main concern, the feasibility of the magnetic recycling of the prepared nanocatalyst was also examined for the preparation of 7-amino-6-cyano-5-(phenyl)-5*H*-pyrano[2,3-*d*]pyrimidine-2,4(1*H*,3*H*)-diones and 2-amino-4-(phenyl)-4,5-dihydro-5-oxopyrano[3,2-*c*]chromene-3-carbonitrile under heating conditions. The nanocatalyst was isolated by a magnet bar without tedious workup, and no centrifugation or filtration step was required. The separated magnetic solid was washed with hot ethanol and dried in vacuum at 60°C. The efficiency of the recovered $CoFe_2O_4$@FA-Er up to six continuous runs is shown in Figure 7a,b. In order to confirm the efficiency of the prepared heterogeneous catalyst, the catalyst turnover frequency (TOF) was calculated as an important factor used for measuring the capability of the catalysts. As indicated in Figure 7c,d, the corresponding product was obtained exclusively with high TOF.

3.5 | Catalyst leaching study

The value of Er leaching in the synthesis of pyrano[2,3-*d*]pyrimidinone was investigated by comparing the metal anchoring value before and after recovering of the catalyst by ICP-OES method. Result showed that the value of Er in intact MNPs and the reused one after six times is 0.49 and 0.46 mmol/g, respectively, which illustrated the minimal Er leaching in the catalytic procedure which demonstrated the efficiency and stability of the catalyst.

3.6 | Hot filtration test

In the last step of current protocol, performance of the introduced catalyst was examined with hot filtration

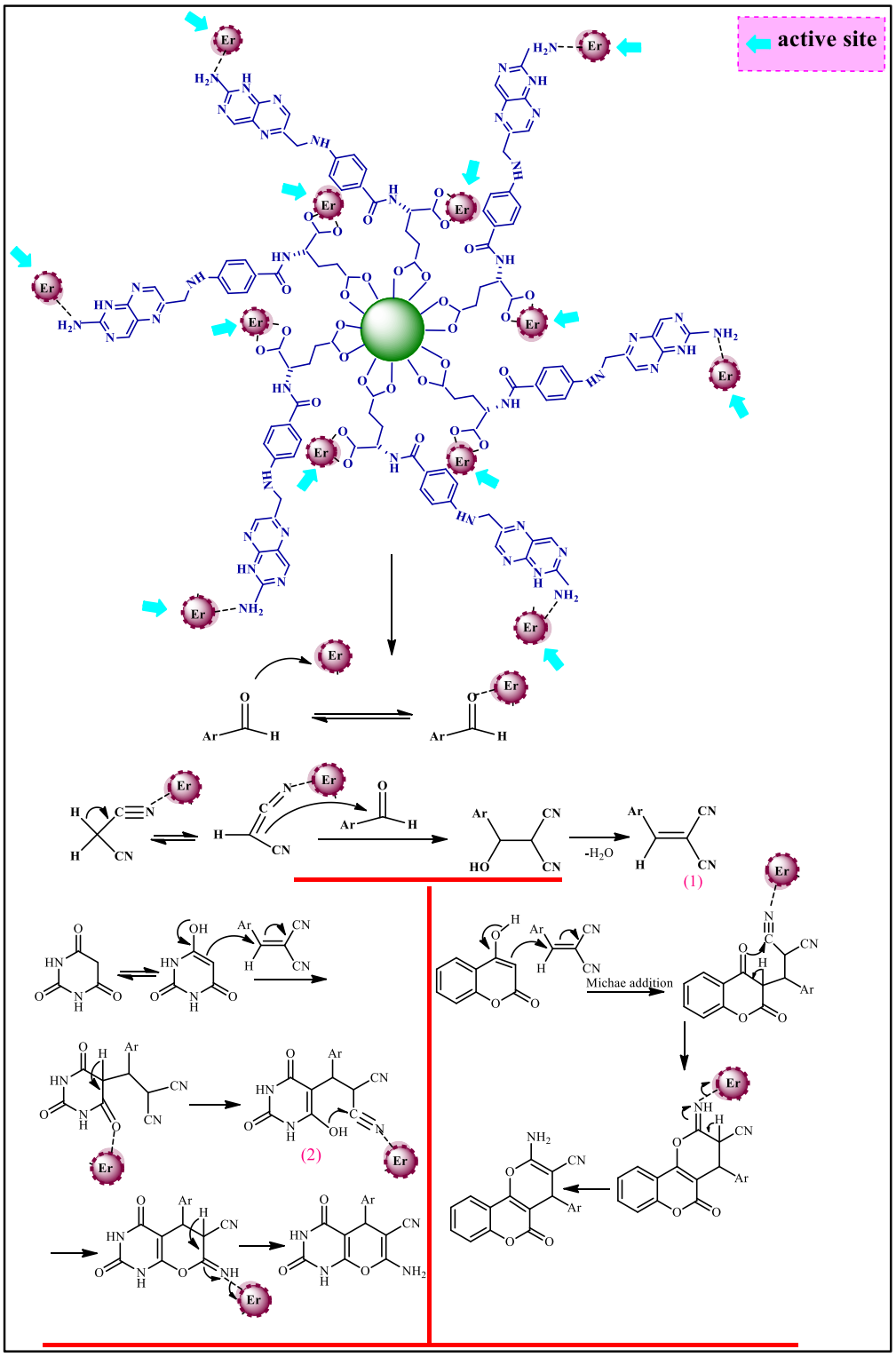

SCHEME 3 Proposed mechanism for the synthesis of pyrano[2,3-*d*]pyrimidinone and dihydropyrano[3,2-*c*] chromenes in the presence of $CoFe_2O_4$@FA-Er magnetic nanoparticles (MNPs)

test. Synthesis of the 2-amino-4-(phenyl)-5-oxo-4*H*,5*H*-pyrano[3,2-*c*]chromene-3-carbonitrile in the presence of reported catalyst was chosen for hot filtration test. Under optimized conditions, the reaction proceeded in the presence of $CoFe_2O_4$@FA-Er in which the product yield was 67% in the half time of the reaction. Then, the reaction was replicated, and the nanocatalyst was isolated in half time of the reaction. Thereupon, the reaction continued without $CoFe_2O_4$@FA-Er in which the yield of reaction was 71%. These considerations corroborated that the leaching of metal has not been happened.

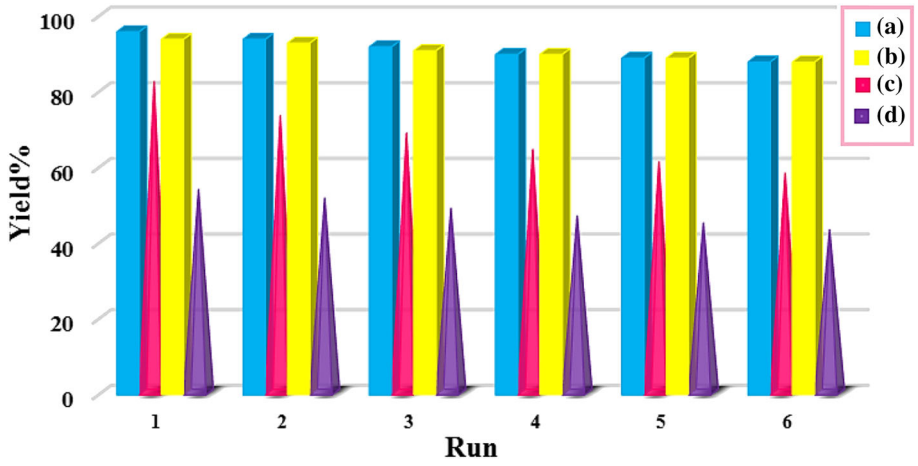

FIGURE 7 Recyclability of the $CoFe_2O_4$ @FA-Er in the synthesis of (a) 7-amino-6-cyano-5-(phenyl)-5*H*-pyrano[2,3-*d*]pyrimidine-2,4(1*H*,3*H*)-diones and (b) 2-amino-4-(phenyl)-4,5-dihydro-5-oxopyrano[3,2-*c*]chromene-3-carbonitrile and turnover frequency (TOF) of (c) 7-amino-6-cyano-5-(phenyl)-5*H*-pyrano[2,3-*d*]pyrimidine-2,4(1*H*,3*H*)-diones and (d) 2-amino-4-(phenyl)-4,5-dihydro-5-oxopyrano[3,2-*c*]chromene-3-carbonitrile after several cycles. TOF = [(mol amount of product)/(mol amount of used catalyst) × (time)]

4 | CONCLUSION

In summary, we have synthesized an efficient magnetic Er immobilized nanocatalyst using FA as green linker for the first time. The heterogeneous $CoFe_2O_4$@FA-Er was easily synthesized and fully characterized by various techniques including FE-SEM, TEM, EDX, X-ray atomic mapping, TGA, XRD, VSM, ICP-OES, and FT-IR spectroscopy. Then, the described nanomagnetic particles were used as novel and inexpensive nanomagnetic catalyst to accelerate the preparation of pyrano[2,3-*d*]pyrimidinone and dihydropyrano[3,2-*c*]chromenes compounds under the sonication conditions or the solvent-free condition at 80°C in H_2O as eco-friendly solvent. This nanocatalyst could be recovered easily by an appropriate external magnet and reused at least six times without significant loss of its catalytic activity. Also, other significant properties of the introduced novel protocol are short reaction times, high catalytic activity, high purity of the products, efficient, and easy workup procedure and progress of the reaction in a green condition.

ACKNOWLEDGMENT

We gratefully acknowledge the support of this work by University of Kurdistan.

AUTHOR CONTRIBUTIONS

Serve Sorkhabi: Conceptualization; data curation; formal analysis; funding acquisition; investigation; methodology; project administration; resources; software; supervision; validation; visualization. **Roya Mozafari:** Conceptualization; data curation; formal analysis; funding acquisition; investigation; methodology; project administration; resources; software; supervision; validation; visualization. **Mohammad Ghadermazi:** Conceptualization; data curation; formal analysis; funding acquisition; investigation; methodology; project administration; resources; software; supervision; validation; visualization.

ORCID

Serve Sorkhabi https://orcid.org/0000-0003-0980-9933
Roya Mozafari https://orcid.org/0000-0002-7621-0528
Mohammad Ghadermazi https://orcid.org/0000-0001-8631-6361

REFERENCES

[1] N. Isambert, M. M. S. Duque, J. C. Plaquevent, Y. Genisson, J. Rodriguez, T. Constantieux, *Chem. Soc. Rev.* **2011**, *40*, 1347.
[2] a) D. Strubing, H. Neumann, S. Klaus, S. Hubner, M. Beller, *Tetrahedron* **2005**, *61*, 11333; b) A. Davoodnia, M. M. Heravi, L. Rezaei-Daghigh, N. Tavakoli-Hoseini, *Monatsh. Chem.* **2009**, *140*, 1499.
[3] H. S. Haeri, S. Rezayati, E. R. Nezhad, H. Darvishi, *Res. Chem. Intermed.* **2016**, *42*, 4773.
[4] S. Rezayati, M. T. Jafroudi, E. R. Nezhad, R. Hajinasiri, S. Abbaspour, *Res. Chem. Intermed.* **2016**, *42*, 5887.
[5] Z. Abbasi, S. Rezayati, M. Bagheri, R. Hajinasiri, *Chin. Chem. Lett.* **2017**, *28*, 75.
[6] S. Rezayati, Z. Abbasi, E. R. Nezhad, R. Hajinasiri, A. Farrokhnia, *Res. Chem. Intermed.* **2016**, *42*, 7597.
[7] S. Sajjadifar, S. Rezayati, A. Shahriari, S. Abbaspour, *Appl. Organomet. Chem.* **2018**, *32*, e4172.
[8] B. M. Trost, *Science* **1991**, *254*, 1471.

[9] R. Khanivar, A. Zare, M. Sadeghi-Takallo, *Asian J. Green Chem.* **2021**, *5*, 1.
[10] F. M. Alaa, A. El-Latif, F. F. Ahmed, M. Amira, *Chin. J. Chem.* **2010**, *28*, 91.
[11] a) A. Basso, L. Banfi, R. Riva, G. Guanti, *J. Org. Chem.* **2005**, *70*, 575; b) S. T. Staben, N. Blaquiere, *Angew. Chem., Int. Ed.* **2010**, *49*, 325; c) T. Yue, M. X. Wang, D. X. Wang, G. Masson, J. Zhu, *J. Org. Chem.* **2009**, *74*, 8396; d) N. Ma, B. Jiang, G. Zhang, S. J. Tu, W. Wever, G. Li, *Green Chem.* **2010**, *12*, 1357.
[12] a) R. A. Sheldon, *Pure Appl. Chem.* **2000**, *72*, 1233; b) L. F. Tietze, G. Kettschau, *Springer* **1997**, *189*, 1.
[13] M. Daraie, M. M. Heravi, T. Tamoradi, *ChemistrySelect* **2019**, *4*, 10742.
[14] A. A. Fayed, H. M. Hosni, E. M. Flefel, A. E. Amr, *World J. Chem.* **2009**, *4*, 58.
[15] A. H. F. Abd El-Wahab, *Acta Pharm.* **2002**, *52*, 269.
[16] L. V. G. Nargund, Y. S. R. Reddy, R. Jose, *Indian Drugs* **1991**, *29*, 45.
[17] A. R. Bhat, R. S. Dongre, P. A. Ganie, *Organic & Medicinal Chem IJ* **2017**, *1*(3), 555565.
[18] A. R. Agarwal, N. Ashutosh, P. M. S. Goyal, S. G. Chauhan, *Bioorg. Med. Chem.* **2005**, *24*, 6678.
[19] R. B. Ajmal, S. D. Rajendra, S. S. Rupali, *Int. J. Pharm. Biosci.* **2014**, *5*, 422.
[20] L. R. Bennett, C. J. Blankely, R. W. Fleming, R. D. Smith, D. K. Tessonam, *J. Med. Chem.* **1981**, *24*, 382.
[21] a) A. D. Broom, J. L. Shim, G. L. Anderson, *J Org Chem* **1976**, *41*, 1095; b) E. M. Grivsky, S. C. Lee, W. Sigel, D. S. Duch, C. A. Nichol, *J. Med. Chem.* **1980**, *23*, 327.
[22] L. Bonsignore, G. Loy, D. Secci, A. Calignano, *Eur. J. Med. Chem.* **1993**, *28*, 517.
[23] Y. Gao, S. Tu, T. Li, X. Zhang, S. Zhu, F. Fang, D. Shi, *Synth. Commun.* **2004**, *34*, 1295.
[24] M. K. A. Ibrahim, M. R. H. El-Moghayar, M. A. F. Sharaf, *Indian J Chem. Sect. B.* **1987**, *26B*, 216.
[25] C. S. Konkoy, D. B. Fick, S. X. Cai, N. C. Lan, J. F. W. Keana, In PCT Int. Appl. WO 0075123(2000), *Chem. Abstr.* **2001**, *134*, 29313a.
[26] F. Mohamadpour, J. Saudi, *Chem. Soc.* **2020**, *24*, 636.
[27] S. Poola, M. S. Shaik, M. Sudileti, S. Yakkate, V. Nalluri, A. Chippada, S. R. Cirandur, *J. Chin. Chem. Soc.* **2020**, *67*, 805.
[28] S. Darvishzad, N. Daneshvar, F. Shirini, H. Tajik, *J. Mol. Struct.* **2019**, *1178*, 420.
[29] N. Daneshvar, M. Nasiri, M. Shirzad, M. S. N. Langarudi, F. Shirini, H. Tajika, *New J. Chem.* **2018**, *42*, 9744.
[30] E. Ezzatzadeh, F. Sheikholeslami-Farahani, K. Yadollahzadeh, S. Rezayati, *Comb. Chem. High Throughput Screening* **2020**, *23*, 1.
[31] V. Pagore, V. Jadhav, P. Bajad, R. Pawar, *Asian J. Green Chem.* **2020**, *4*, 379.
[32] S. Sajjadifar, Z. Gheisarzadeh, *Appl. Organomet. Chem.* **2018**, *33*, e4602.
[33] M. E. Sedaghat, M. Rajabpour Booshehri, M. R. Nazarifar, F. Farhadi, *Appl. Clay Sci.* **2014**, *95*, 55.
[34] N. N. Pesyan, G. R. Bardajee, E. Kashani, M. Mohammadi, H. Batmani, *Res. Chem. Intermed.* **2020**, *46*, 347.
[35] H. Shahbazi-Alavi, A. Kareem Abbas, J. Safaei-Ghomi, *Nano* **2020**, *2*, 56.
[36] A. Akbari, *Heterocycl. Commun.* **2013**, *19*, 425.
[37] H. Nagabhushana, S. Sandeep Saundalkar, L. Muralidhar, B. M. Nagabhushana, C. R. Girija, D. Nagaraja, M. A. Pasha, V. P. Jayashankara, *Chin. Chem. Lett.* **2011**, *22*, 143.
[38] H. Mehrabi, M. Kazemi-Mireki, *Chin. Chem. Lett.* **2011**, *22*, 1419.
[39] S. Sorkhabi, M. Ghadermazi, R. Mozafari, *RSC Adv.* **2020**, *10*, 41336.
[40] M. Miranzadeh, F. Afshari, B. Khataei, M. Kassaee, *Adv. J. Chem. A.* **2020**, *3*, 408.
[41] I. Amar, Z. Alshibani, M. AbdulQadir, I. Abdalsamed, F. Altohami, *Adv. J. Chem. A.* **2019**, *2*, 365.
[42] H. Noorizadeh, A. Farmany, *Adv. J. Chem. A.* **2019**, *2*, 128.
[43] T. Tamoradi, A. Ghorbani-Choghamarani, M. Ghadermazi, *Polyhedron* **2018**, *145*, 120.
[44] S. Shylesh, V. Schunemann, W. R. Thiel, *Chem. – Eur. J.* **2010**, *16*, 8950.
[45] M. Esmaeilpour, J. Javidi, F. NowrooziDodeji, M. Mokhtari Abarghoui, *J. Mol. Catal. A: Chem.* **2014**, *393*, 18.
[46] T. Tamoradi, A. Taheri, S. Vahedi, M. Ghadermazi, *Solid State Sci.* **2019**, *97*, 105981.
[47] R. Mozafari, F. Heidarizadeh, *Polyhedron* **2019**, *162*, 263.
[48] R. Mozafari, M. Ghadermazi, *RSC Adv.* **2020**, *10*, 15052.
[49] T. Tamoradi, A. Ghorbani-Choghamarani, M. Ghadermazi, *Solid State Sci.* **2019**, *88*, 81.
[50] A. Kalam, A. G. Al-Sehemi, M. Assiri, G. Du, T. Ahmad, I. Ahmad, M. Pannipara, *Results in Physics* **2018**, *8*, 1046.
[51] B. Stella, S. Arpicco, M. T. Peracchia, D. Desmaële, J. Hoebeke, M. Renoir, *J. Pharm. Sci.* **2000**, *11*, 1452.
[52] M. A. Caudill, J. F. Gregory, A. D. Hutson, L. B. Bailey, *J. Nutr.* **1998**, *128*, 204.
[53] T. Tamoradi, S. M. Mousavi, M. Mohammadi, *New J. Chem.* **2020**, *44*, 8289.
[54] T. Tamoradi, S. M. Mousavi, M. Mohammadi, *New J. Chem.* **2020**, *44*, 3012.
[55] T. Tamoradi, M. Daraie, M. M. Heravi, B. Karmakar, *New J. Chem.* **2020**, *44*, 11049.
[56] B. Zamani-Ranjbar-Garmroodi, M. A. Nasseri, A. Allahresani, K. Hemmat, *Res. Chem. Intermed.* **2019**, *45*, 5665.
[57] A. R. Jalilian, S. L. Hosseini-Salekdeh, M. Mahmoudi, H. Yousefnia, A. Majdabadi, M. Pouladian, *J. Radioanal. Nucl. Chem.* **2011**, *287*, 119.
[58] A. Shaabani, S. Samadi, A. Rahmati, *Synth. Commun.* **2007**, *37*, 491.
[59] M. M. Heravi, A. Ghods, K. Bakhtiari, F. Derikvand, *Synth. Commun.* **2010**, *40*, 1927.
[60] M. Bararjanian, S. Balalaie, B. Movassagh, A. M. Amani, *J Iran Chem Soc.* **2009**, *6*, 436.
[61] A. Khazaei, A. Ranjbaran, F. Abbasi, M. Khazaei, A. R. Moosavi-Zare, *RSC Adv.* **2015**, *5*, 13643.
[62] S. Abdolmohammadi, S. Balalaie, *Tetrahedron Lett.* **2007**, *48*, 3299.
[63] A. Hasaninejad, M. Shekouhy, N. Golzar, A. Zare, M. M. Doroodmand, *Appl. Catal. A: General* **2011**, *402*, 11.
[64] J. Wang, D. Shi, Q. Zhuang, X. Wang, H. Hu, *J. Chem. Res.* **2004**, *2004*, 818.
[65] M. G. Dekamin, M. Eslami, A. Maleki, *Tetrahedron* **2013**, *69*, 1074.

[66] S. Paul, S. Ghosh, P. Bhattacharyy, A. R. Das, *RSC Adv.* **2013**, *3*, 14254.
[67] K. Niknam, A. Jamali, *Chin. J. Catal.* **2012**, *33*, 1840.
[68] G. Mohammadi Ziarani, A. Badiei, M. Azizi, P. Zarabadi, *Iran. J. Chem. Chem. Eng.* **2011**, *30*, 59.
[69] E. Jahangarda, L. Khazdooza, A. Zarei, *Iran. J. Catal.* **2020**, *10*, 57.
[70] R. Karimi-Chayjani, N. Daneshvar, H. Tajik, F. Shirini, *ChemistrySelect* **2019**, *4*, 1205.
[71] H. J. Wang, J. Lu, Z. H. Zhang, *Monatsh. Chem.* **2010**, *141*, 1107.

How to cite this article: Sorkhabi S, Mozafari R, Ghadermazi M. New advances in catalytic performance of erbium-folic acid-coated $CoFe_2O_4$ complexes for green one-pot three-component synthesis of pyrano[2,3-*d*]pyrimidinone and dihydropyrano[3,2-*c*]chromenes compounds in water. *Appl Organomet Chem*. 2021;e6225. https://doi.org/10.1002/aoc.6225